A Semi-Heuristic Approach for Tracking Buried Subsea Pipelines using Fluxgate Magnetometers

A Semi-Heuristic Approach for Tracking Buried Subsea Pipelines using Fluxgate Magnetometers

Vibhav Bharti, David Lane and Sen Wang[1]

***Abstract*— Integrity assessment of subsea oil and gas transmission lines is crucial for safe and environment-friendly operations. These are usually very expensive without employing Autonomous Underwater Vehicles (AUVs). Buried sections of long pipelines pose a major hurdle in effective pipeline tracking through an AUV. If a pipe track is lost, then the vehicle needs to invest resources to relocate the pipeline. This work presents a heuristic-based method to detect buried pipes using magnetometers followed by a Kalman filter parameterized to optimally localize subsea pipes. Extensive experiments on real and simulated data are conducted to show the reliable performance of this method for tracking buried pipelines.**

I. Introduction

One of the major benefactors of underwater automation technology is Oil & Gas industry [1] for inspection of offshore infrastructure. Assessment of these assets is vital for ensuring safety and continuity of operation, devising an action plan for repairs or disaster mitigation. Field robotics plays a key role in automating this process, making it more efficient and cost-effective. Autonomous Underwater Vehicles (AUVs) are favourable for long-range offshore survey operations as they are more flexible than cable controlled Remotely Operated Vehicles (ROVs) and do not require an expensive surface support vessel. A well-established commercial application of this is subsea pipeline tracking, where an AUV follows a target pipe over long ranges [2].

The prime objective of these surveys is to gather inspection data that can be viewed real-time dependent on communication limits or analysed later. Detection and tracking of exposed subsea pipes are well studied in literature and industry alike. There are many methodologies available for this using imaging sonars, profiling sonars or video cameras. Sidescan sonar is more convenient for covering large areas at longer ranges and higher speeds. A combination of sidescan at long range for initial detection and multibeam echosounder (MBE) at short range was successfully demonstrated in AUTOTRACKER project [3].

An AUV has to fly close to the target pipeline to collect quality survey data. A key challenge in tracking subsea pipelines is when sections of pipes are buried and not detected in visual or acoustic sensors. Thus, when the pipeline goes into burial and pipe track is lost, AUV either goes at higher altitude to relocate the pipeline in sidescan sonar or it may have to resurface for a GPS fix and then use historical information on pipeline's location. Possible solutions for detecting buried pipelines is either sub-bottom profilers (SBP) or using magnetometers as most subsea pipes are ferromagnetic. However, processing both these modalities is not as straightforward as with visual and high-frequency sonars. The main benefit of using a magnetometer is power savings as SBP tends to require more power to be able penetrate seabed surface.

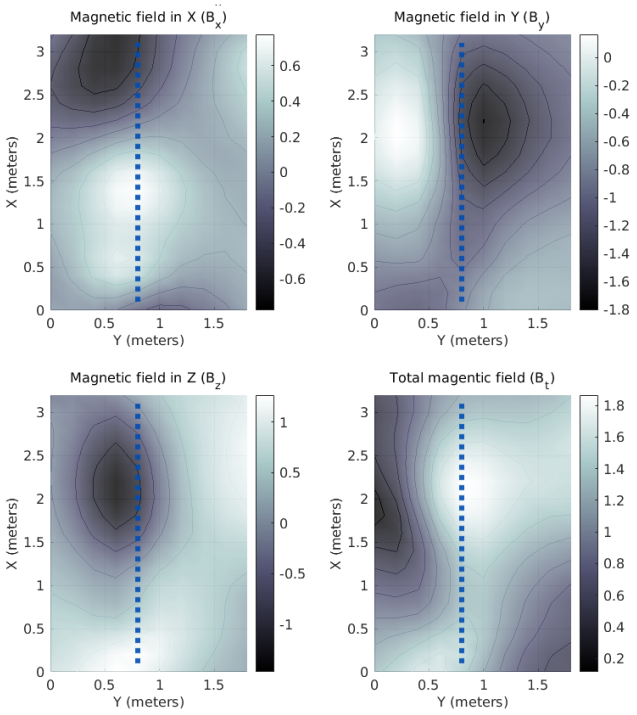

(a) Contour plot of magnetization (microtesla, μT) for test pipe (blue line) with magnetometer oriented same way as the axis.

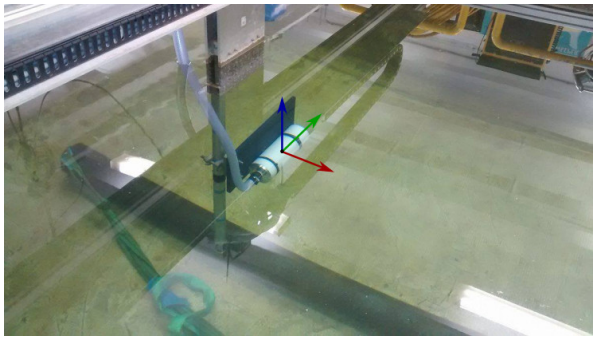

(b) A 3m length, 6 inch SCH 40 A106 Grade B Seamless Pipe for test analysis in Ocean Systems Lab water tank.

Fig. 1: Grid analysis of magnetic field density of a ferromagnetic pipe using a fluxgate magnetometer.

[1]All authors are with School of Physical and Engineering Sciences, Heriot-Watt University, Edinburgh EH141NF, United Kingdom {vb97,d.m.lane, s.wang}@hw.ac.uk

(a) (b) (c)

Fig. 2: Sensor set lowered in dock (left). Collection of data with sensors attached to C-Enduro ASV (middle). Simulation in UWsim with a pipe going from fully exposed to buried with simulated magnetometers [4] (right).

In this work, we present a novel approach for tracking buried pipelines using two fluxgate magnetometers. The approach is divided into heuristic-based detection followed by an Extended Kalman filter to track/localize the target pipe and thus take appropriate control action. We also suggest suitable strategy for using proposed algorithm to keep optimum attitude with the pipe. To the best of our knowledge, this is the first work demonstrating successful tracking of buried pipelines using only fluxgate magnetometers.

The rest of the papers in organized in following order: In section II, we review relevant works about pipeline detection using magnetometers, we describe the method in section III and IV and we present our experiments and results on real and simulated data in section V.

II. Background

It is common knowledge in domain of material science that magnetic intensity of ferromagnetic materials increases significantly in presence of external magnetic fields and that this effect is also produced by Earth's geomagnetism. Any pipeline is going to produce additional magnetism from this in addition to its own permanent magnetization. Thus, a magnetic probe taking measurements around a ferromagnetic pipe will produce considerable magnetic anomaly in geomagnetic field. This property of subsea pipes can be exploited for its detection using magnetometers [5], [6].

A pipeline under the influence of geomagnetism will show different magnetic anomalies depending on direction of the geomagnetic field. Since a pipeline is long axially, the magnetization due to axial component of pipe is going to be low [7]. Which means that a long pipe can be considered as a line of dipoles whose total magnetic field intensity is inversely proportional to squared distance from sensor to the pipe [5]. Breiner [5] has also suggested that to get detection, it is best to perform traverses perpendicular to the target pipe accept when pipe is aligned to north-south at equator due to mostly axial magnetism of low magnitude. The method of horizontal traverses is extended to develop an algorithm able to compute orientation of the pipe by Zhao et. al. [7], however requires a large grid of magnetometer data for it.

To the best of our knowledge, there is very little literature specifically targeting the problem of tracking pipes using magnetometers mounted on an underwater vehicle. It is partially due to the challenge in processing and inferring information from magnetometer data while vehicle is in forward motion along the pipe. Tian [8] has used a combination of magnetometer and sub-bottom profiling (SBP) sonar to detect the pipeline and has added that this approach cannot tell the difference between a exposed or buried pipe. In his design, the sensor is towed to avoid the magnetic signatures of the AUV itself. However, his method relies more on using sub-bottom profiler than the magnetometer. Naeem et al. [9] have also mentioned that lateral and longitudinal displacement is obtainable using magnetic sensors, but it is not possible to obtain orientation while tracking with limited non-grid sensors.

Detection using magnetometer is not easy due to highly non-linear nature of magnetic field produced by series of pipes welded together. Indeed in our real data, we had very variable data either due to considerable permanent magnetization of pipe or due to location (see figures 1a, 8 and 9). Range can be calculated only if parameters for the exact models are available and magnetization in pipe is strictly aligned to geomagnetism.

III. Detection

Magnetic field anomaly produced by ferromagnetic pipes is highly ambiguous. This is also evident by the real data we have collected (see Figure 8 and 9). Thus, it best to design an algorithm under assumption of arbitrary magnetization, which makes the method generic to be applied to any pipeline without prior knowledge.

A. Compensating Geomagnetism

The magnetic reading taken by the 3-axis magnetometer measures the total magnetic field at sensor's location. This reading includes the geomagnetic field of Earth and needs to be removed in order to obtain fields generated by target pipe. Geomagnetic field can either be pre-measured at a known location in absence of other magnetic objects or using World Magnetic Model (WMM) [10] at any geographic coordinate.

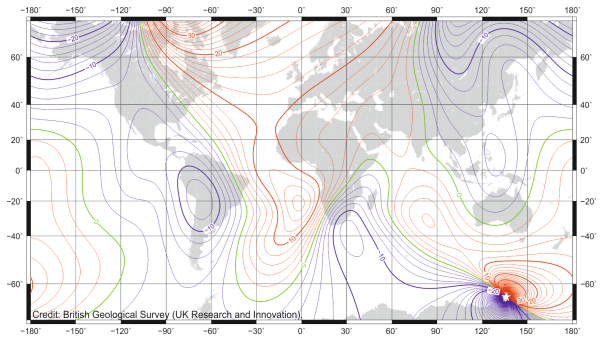

Fig. 3: Geomagnetic plot using World Magnetic Model (image credits: British Geological Survey).

These values also do not change drastically over short distances and thus doesn't need to be computed often and can be calculated on ad-hoc basis. WMM takes geo-coordinates (Latitude and longitude), altitude and date as input and gives all the geomagnetic components at any location on Earth. Thus, we obtain total field, northing, easting, vertical and horizontal components represented by G_F, G_N, G_E, G_V and G_H respectively. A plot of geomagnetism using WMM is presented in Figure 3.

For taking magnetic readings, the x-y plane is usually tangential and z-axis normal to Earth's surface. To calculate the effect of geomagnetism on sensor readings, the vehicle's bearing with respect to geographic north at any given time needs to be taken into account. Consider the bearing of the vehicle, θ, then the effect of geomagnetic northing and easting on the sensor can be computed by applying following rotation matrix,

$$\begin{bmatrix} G_y \\ G_x \end{bmatrix} = \begin{bmatrix} \cos\theta & -\sin\theta \\ \sin\theta & \cos\theta \end{bmatrix} \times \begin{bmatrix} G_E \\ G_N \end{bmatrix} \tag{1}$$

Thus, the magnetic field ($\mathbf{B}_p$) produced by pipeline can be calculated by subtracting effects geomagnetic field at given vehicle yaw, θ. If the raw magnetic field reading taken by sensor is given as $\mathbf{B}_g = [B_{g,x}\ B_{g,y}\ B_{g,z}]$, then, compensated magnetic field can be computed as,

$$\mathbf{B}_p = \begin{bmatrix} B_x \\ B_y \\ B_z \\ B_a \end{bmatrix} = \begin{bmatrix} B_{g,x} - G_x \\ B_{g,y} - G_y \\ B_{g,z} - G_V \\ B_{g,t} - G_F \end{bmatrix} \tag{2}$$

where, B_a is the total magnetic anomaly, and total magnetic field $B_t = \sqrt{B_x^2 + B_y^2 + B_z^2}$ is calculated as combined magnitude of geo-compensated 3-axes readings.

B. Heuristics-Based Detection

For arbitrary magnetization, it is best to use total magnetic field of the target object, B_t. The existence of pipe is established by considering the total magnetic noise level at the offshore location modelled by a Gaussian distribution $\mathcal{N}(\mu_B, \sigma_B)$. The noise variance σ_B can be calculated at earlier stage when there are no magnetic objects in the surrounding area. Thus, with a single sensor we could establish existence of a magnetic object at vehicle's current location by setting a heuristic threshold on total magnetic field, $B_{thresh} = \mu_B + 3\sigma_B$.

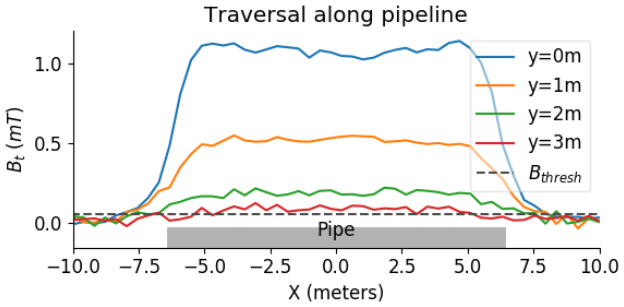

(a) Variation in field as vehicle move along pipe.

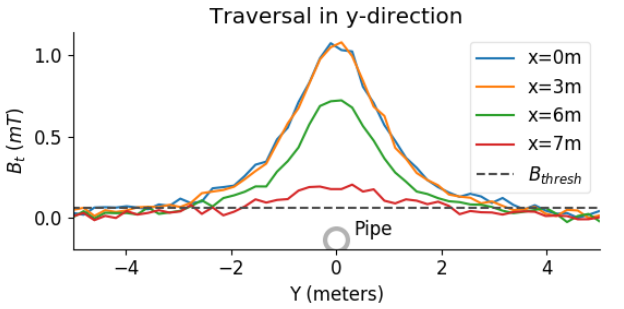

(b) Variation in field as vehicles sways sideways.

Fig. 4: Simulated total magnetic field as the sensor traverses in difference directions. In both cases, sensor is aligned parallel to the pipe at height of $z = 1m$ (sensor x-y plane aligned to x-y of coordinate system).

Figure 4 shows example of this where we have simulated the magnetic field of a pipe of length $12m$ placed at the origin, magnetized vertically with added noise. With the sensor aligned to the coordinate axis, readings are simulated at constant height of $z = 1m$ for when the sensor is moving along the pipe (Figure 4a) and when the vehicle is moving sideways (Figure 4b).

A binary detection is made when total magnetic field is larger than the peak noise level, $B_t > B_{thresh}$. This can be used in succession as the vehicle moves and then with sway manoeuvres, we are able to follow the pipe heuristically. However, this going to put more load and rely heavily on vehicle planner and controller. For improving these detections, we propose using two sensors instead, one on each side of the vehicle. With two sensors, four detection states can be obtained instead of two at each timestep: [Center, Left, Right, None].

Denoting the total magnetic field observed by the pipes on each side by $B_{t,L}$ $B_{t,R}$ for left and right sensor respectively. Then detection can be obtained by using Algorithm 1, where a detection is obtained by calculating the ratio between total magnetic field of both sensors. Now we would need another threshold to set detection states (centred, left or right) based on ratio given by B_{rth}. The value for B_{rth} can be calibrated using average detections from visual or profiling sensors such as multibeam tracking method presented in [11].

IV. TRACKING

The system is under-observed from limitations of magnetometer-based detection algorithm. The measurements are made on a 2D plane (x-y plane of AUV) as while tracking the vehicle does not pitch or roll and proposed detection algorithm is not able to infer depth (z-axis). Thus, estimating full 3D location would not be possible. Another major limitation of detection algorithm is that only centre detections can be used for filtering process as left or right detections cannot be modelled.

Under these conditions, an Extended Kalman Filter is formulated to track from 2D observations. This will also estimate pipe's orientation which is very desirable for this application. The Kalman state vector thus consists of 2D position and orientation of the pipe, $\mathbf{x}_k = [x_k \ y_k \ \psi_k]^T$.

A. Prediction Model

For previous state $\mathbf{x}_{k-1}$ at timestep $k-1$, the current state is given using following equation,

$$\mathbf{x}_k = f\big(\mathbf{x}_{k-1}\big) + \mathbf{w}_k \tag{3}$$

where $f(\mathbf{x}_k)$ is the non-linear prediction model and is given by,

$$f(\mathbf{x}_k) = \begin{bmatrix} x_k + d_k.\cos\psi_k \\ y_k + d_k.\sin\psi_k \\ \psi_k \end{bmatrix} \tag{4}$$

and $\mathbf{w}_k \sim \mathcal{N}\big(\mathbf{0}, \mathbf{Q}_k\big)$ is the associated prediction noise assumed as zero-mean Gaussian with covariance matrix $\mathbf{Q}_k$ and d_k is distance of pipe traversed from previous timestep to current timestep. It is better computed in vector form to account for reverse motions. If pipe is described as a line, $L_{pipe} : \mathbf{X}_k + d_k\vec{\mathbf{V}}_k$ with a previous pipe point, $\mathbf{X}_k = [x_k \ y_k]$ and direction vector, $\vec{\mathbf{V}}_k = [\cos(\psi_k) \ \ \sin(\psi_k)]$, then d_k is given by following dot product,

$$d_k = \langle \mathbf{X}_k, \vec{\mathbf{V}}_k \rangle \tag{5}$$

To propagate the error covariance of Kalman filter, the non-linear motion model needs to be linearised by computing Jacobian of $f(\mathbf{x}_k)$ with respect to state variables. This is given as,

$$\mathbf{F}_k = \begin{bmatrix} \frac{\partial f_1}{\partial x_p} & \frac{\partial f_1}{\partial y_p} & \frac{\partial f_1}{\partial \psi_p} \\ \frac{\partial f_2}{\partial x_p} & \frac{\partial f_2}{\partial y_p} & \frac{\partial f_2}{\partial \psi_p} \\ \frac{\partial f_3}{\partial x_p} & \frac{\partial f_3}{\partial y_p} & \frac{\partial f_3}{\partial \psi_p} \end{bmatrix} = \begin{bmatrix} 1 & 0 & -d_k \cdot sin\psi_k \\ 0 & 1 & d_k \cdot cos\psi_k \\ 0 & 0 & 1 \end{bmatrix} \tag{6}$$

Pipeline tracking is performed in vehicle's coordinate frame, thus previous estimate needs to be transformed to compensate for vehicle's motion. Hence, we obtain the homogeneous coordinate transformation matrix from vehicle's previous to current position from vehicle's navigation module and is given by translation vector ${}^k\mathbf{T}_{k-1}$ for change in position and square rotation matrix ${}^k\mathbf{R}_{k-1}$ is for change in vehicle's rotation from previous timestep. This will also include noise covariance matrix, $\mathbf{Q}_k$ which is the difference between current and previous pose covariance. This will be the added noise in Kalman filter as it's mostly from vehicle's motion. Thus if the state estimate at previous frame is $\hat{\mathbf{x}}_{k-1}^{prev} = [x_{k-1}^{prev} \ y_{k-1}^{prev} \ \psi_{k-1}^{prev}]$ (superscript ^{prev} referring to estimate in previous frame), then

$$\hat{\mathbf{x}}_{k-1} = \begin{bmatrix} x_{k-1} \\ y_{k-1} \\ \psi_{k-1} \end{bmatrix} = \begin{bmatrix} {}^k\mathbf{R}_{k-1} \begin{bmatrix} x_{k-1}^{prev} \\ y_{k-1}^{prev} \end{bmatrix} + {}^k\mathbf{T}_{k-1} \\ \psi_{k-1}^{prev} + \Delta\theta \end{bmatrix} \tag{7}$$

where, $\Delta\theta$ is change in vehicle's yaw obtained from rotation matrix ${}^kR_{k-1}$.

B. Observation Model

The observation model is built around the limitations of detection algorithm and models its behaviour optimally. Since only centre detection can be accurately modelled, the filter is said to make an observation only when the vehicle

Algorithm 1 Detection Algorithm

Input: Geo-compensated total magnetic fields, $B_{t,L}$ and $B_{t,R}$
Output: Detection , D_k
Initialize: $D_k =$ 'None'
if ($B_{t,L} > B_{thresh}$ & ($B_{t,R} > B_{thresh}$) **then**
  $B_{ratio,L} = \frac{B_{t,L}}{(B_{t,L}+B_{t,R})}$
  $B_{ratio,R} = \frac{B_{t,R}}{(B_{t,L}+B_{t,R})}$
  if $B_{ratio,L} > B_{rth}$ **then**
    $D_k =$ 'Left'
  else if $B_{ratio,R} > B_{rth}$ **then**
    $D_k =$ 'Right'
  else
    $D_k =$ 'Center'
  end if
end if
return D_k

B_{thresh} is the threshold for binary detection in single magnetometer and B_{rth} is the ratio threshold for detecting centre, left or right.

Algorithm 2 Tracking Algorithm

Input: Previous estimate $\hat{\mathbf{x}}_{k-1}$ and detection D_k
Output: $\hat{\mathbf{x}}_k$
$\hat{\mathbf{x}}_{k|k-1} = f(\hat{\mathbf{x}}_{k-1})$
$\mathbf{P}_{k|k-1} = \mathbf{F}_k\mathbf{P}_{k-1}\mathbf{F}_k^{'} + \mathbf{Q}_k$
if $D_k ==$ 'Center' **then**
  $\tilde{\mathbf{y}}_k = \mathbf{z}_k - \mathbf{H}_k\hat{\mathbf{x}}_{k|k-1}$
  $\mathbf{S}_k = \mathbf{R}_k + \mathbf{H}_k\mathbf{P}_{k|k-1}\mathbf{H}_k^{'}$
  $\mathbf{K}_k = \mathbf{P}_{k|k-1}\mathbf{H}_k^{'}\mathbf{S}_k^{-1}$
  $\hat{\mathbf{x}}_k = \hat{\mathbf{x}}_{k|k-1} + \mathbf{K}_k\tilde{\mathbf{y}}_k$
  $\mathbf{P}_k = (\mathbf{I} - \mathbf{K}_k\mathbf{H}_k)\mathbf{P}_{k|k-1}$
end if
return $\hat{\mathbf{x}}_k$

$z_k = [0 \ 0]'$ is the observation and is assumed to be taken at vehicle's current position, $\tilde{y_k}$ is the innovation, S_k is the innovation covariance and K_k is the Kalman gain.

is above the pipeline. This also means that the observation, z_k, is always equal to $[0,\ 0]^T$. The observation model $h(\mathbf{x}_k)$ maps the state vector, $\mathbf{x}_k$, to observation space and gives observation $\mathbf{z}_k$,

$$\mathbf{z}_k = h\big(\mathbf{x}_k\big) + \mathbf{v}_k \tag{8}$$

where $\mathbf{v}_k \sim \mathcal{N}\big(\mathbf{0}, \mathbf{R}_k\big)$ is the zero-mean Gaussian observation noise with covariance matrix $\mathbf{R}_k$. Since the observation is linear, observation matrix is given in discrete form as,

$$\mathbf{H}_k = \begin{bmatrix} 1 & 0 & 0 \\ 0 & 1 & 0 \end{bmatrix} \tag{9}$$

Observation noise, R_k needs to model the behaviour of detection algorithm properly to provide an optimal estimate of pipe's location. Thus the observation noise, $\sigma^2_{v_k}$, is function of ratio parameter, B_{rth}, that was used in detection algorithm.

$$\mathbf{R}_k = \max(\frac{1}{d_k}, 1) \times \sigma^2_{v_k} \times \mathbf{I}_{3\times 3} \tag{10}$$

The factor $\max(d_k^{-1}, 1)$ also needs to be multiplied to observation noise to avoid converging to single point when vehicle is stationary or when it is moving very short distance. This implies that for a stationary vehicle, the estimate will not change as observation noise covariance tends to infinity. Algorithm 2 describing the Kalman Filter can now be used to recursively estimate target pipe with $\hat{\mathbf{x}}_k$ as the state estimate and $\mathbf{P}_k$ as it's covariance.

C. Observability Analysis

The modelling of the filter is done in such a way that it increases the observability to accurately estimate the state vector. Figure 5 shows strategies to further improve observability to make sure that the filter is able to converge faster even with limitation of detection algorithm.

To validate the modelling and confirm that filter can indeed estimate the state variables, the observability is analysed. An unobservable filter is one where regardless of how many observations are made, the system will not converge to meaningful solution for quantities in the state vector. On the contrary, an observable state vector of size n should start to converge within n observations. Based on [12], the observability matrix for the filter with 3 state variables can be computed as,

$$\mathcal{O} = \begin{bmatrix} \mathbf{H}_k & \mathbf{H}_{k+1} \cdot \mathbf{F}_k & \mathbf{H}_{k+2} \cdot \mathbf{F}_{k+1} \cdot \mathbf{F}_k \end{bmatrix}^T \tag{11}$$

$$\mathcal{O} = \begin{bmatrix} 1 & 0 & 0 \\ 0 & 1 & 0 \\ 1 & 0 & -d_k . \sin\psi_k \\ 0 & 1 & d_k . \cos\psi_k \\ 1 & 0 & -d_{k+1} . \sin\psi_{k+1} - d_k . \sin\psi_k \\ 0 & 1 & d_{k+1} . \cos\psi_{k+1} + d_k . \cos\psi_k \end{bmatrix} \tag{12}$$

For the system to be observable, the observability matrix $\mathcal{O}$ should be of $rank = 3$. To find the rank of the matrix, it needs to be reduced to row echelon form. The reduced form

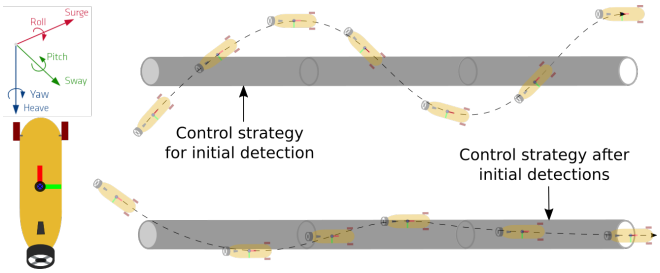

Fig. 5: Strategy to best utilize the tracker using specific manoeuvres while still going along the pipe.

of equation 12 is thus obtained,

$$\mathcal{O} = \begin{bmatrix} 1 & 0 & 0 \\ 0 & 1 & 0 \\ 0 & 0 & T_c \\ \mathbf{0}_{3\times 3} \end{bmatrix} \text{ or } \begin{bmatrix} 1 & 0 & 0 \\ 0 & 1 & 0 \\ 0 & 0 & T_s \\ \mathbf{0}_{3\times 3} \end{bmatrix}$$

where, $T_c = (d_{k+1} . \cos\psi_{k+1} + d_k . \cos\psi_k)$ or $T_s = -(d_{k+1} . \sin\psi_{k+1} + d_k . \sin\psi_k)$. We can draw following conclusions on analysing row echelon form of observability matrix $\mathcal{O}$,

1) Rank of matrix $\mathcal{O}$ is 3 as long $d_k \neq 0$ and $d_{k+1} \neq 0$. Implying that if the vehicle is stationary, then $rank(\mathcal{O}) = 2$ and in stationary vehicle's case the state variables are not observable. This validates the multiplicative factor of $\max(d_k^{-1}, 1)$ in equation 10.
2) Even when the vehicle is moving straight at consistent pace, i.e $d_{k+1} \approx d_k$ and $\psi_{k+1} \approx \psi_k$, since $sin(\psi_k)$ and $cos(\psi_k)$ cannot be equal to 0 at the same time, the rank of observability matrix $\mathcal{O}$ remains 3. This implies that as long as the vehicle manages to keep an alignment with the pipe, the estimate is going to be convergent.

V. Experiments

A. Simulated Data

The algorithm is developed and tested extensively in simulation using Robot Operating System (ROS) as it provided more controlled environment and proper groundtruth. Python library "magpylib" [4] allows for simulating magnetic fields and magnetic sensors in 3D. Magpylib allows to place a pipe in 3D space and then compute the magnetic field at any other 3D location. UWsim package for ROS is used to simulate the vehicle and the scenario is modelled using Blender 3D software and then imported to UWsim. A scenario is created with using 7 pipes sections (see Figure 2c), going from fully exposed to fully buried. Each section is added to the magnetic system of "magpylib". Thus the simulator can generate simulated data directly from the UWsim as the vehicle moves.

B. Real Data

The dataset that we used for real experiments was gathered inside a dry dock at ORE Catapult in Blyth, UK. An underwater environment was arranged to reflect actual scenario with pipes placed at bottom of the dock at an inclination.

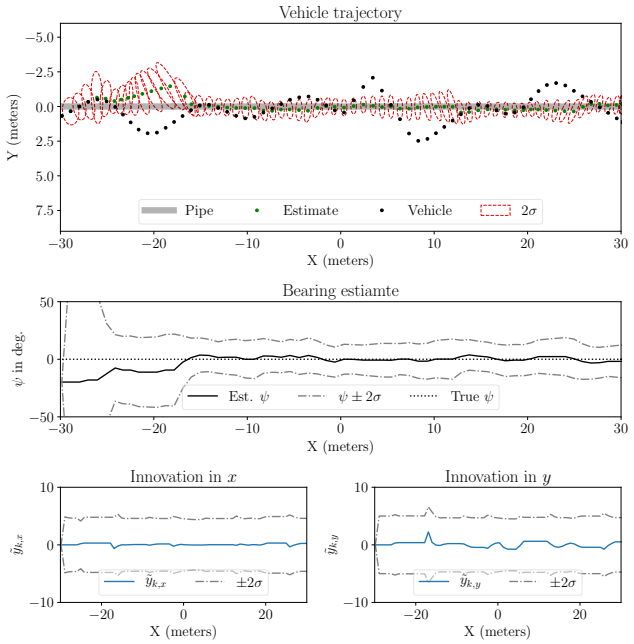

Fig. 6: Tracking results from simulation in UWSim. The tracking filter gets initialized when the AUV crosses pipe the first time. Then after successive detections the filter's estimate converges to right orientation and position of the pipe.

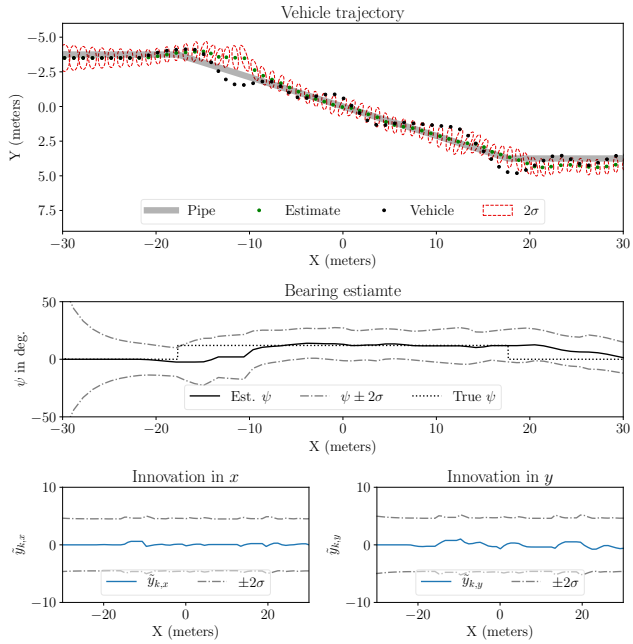

Fig. 7: Simulated tracking result for pipe that turns twice during the run (mid-section at 12^o angle). Such turns may not occur in quick succession in field. However, the tracking algorithm is successfully able to adapt to the turning pipe as more observations are taken.

The dock was levelled out later by adding additional mud and sediments thus creating a setup where the pipe goes from fully exposed to fully buried. The dock was flooded with seawater later. Figure 2a shows the sensor rig at the dock. It was mounted underneath C-Enduro ASV that we have at Ocean Systems Lab in Heriot-Watt University.

The vehicle's GPS data is used for getting the vehicle trajectory. Tracking is performed in a Cartesian frame of reference. The geographic coordinates from AIS/GPS are converted to ECEF (earth-centred, earth-fixed) coordinate system. A homogeneous coordinate transform then is constructed to convert locations to Cartesian (method detailed in [11]).

C. Results

The simulation is made as close to the real data as possible, thus both simulated and real results are generated using same filter parameters. For the detection, the amplitude threshold is set to $B_{thresh} = 5000nT$ and ratio parameter is set to constant value of $B_{rth} = .55$ as the vehicle does change height during the run. Observation noise covariance is the only parameter to be set for the filter. Ideally, this is obtained by calibrating with B_{rth}. However, for the experiments we've set at constant value of $\sigma_{v_k} = 1.414$. The vehicle is manually operated in all cases since vehicle control is out of scope of this paper.

Tracking result from simulation is presented in figure 6 and 7. In figure 6, the AUV crosses the pipeline at angle. The pipe gets detected early on in this simulation, but the filter will not initialize until the detector declare the AUV is centre/above the pipe. The angular covariance is initialized with high value and does not get estimated properly until few crossings are made. Once the angle has converged, the vehicle continues to hold good estimate even when it is far away from the pipe. The strategy shown in 5 is used for this simulation, where the vehicle is first turning and then sways sideways.

In simulated result of figure 7, the pipe turns twice in the run. The vehicle is initially moved along the pipe and when the algorithm encounters a conflict between estimate and detection, then the vehicle prioritizes the detections for its control (manually operated here). The filter starts to converge to the new angle successfully after few crossings.

Consistency of the the Kalman filter is also done for the simulated data and can be seen in figures 6 and 7 with innovation in $\tilde{y}_x$ and $\tilde{y}_y$ and zero-mean standard deviation from $S_{k,(x,x)}$ and $S_{k,(y,y)}$. It can be seen in the plots that the filter is consistent as innovations are not diverging. The jumps happen only when there were no observations for a while.

Figures 8 and 9 shows the results from real data. In both scenarios, vehicle is manually controlled to go over the pipe. In Figure 8, the vehicle moves from the buried section of the pipe. Once the first centre detection is made, the filter is initialized, but since further centre detections are not made, the covariance keeps increasing. Then the filter converges when the detection algorithm outputs centre detection. Figure 9 show the result when vehicle crossed the pipe at an angle

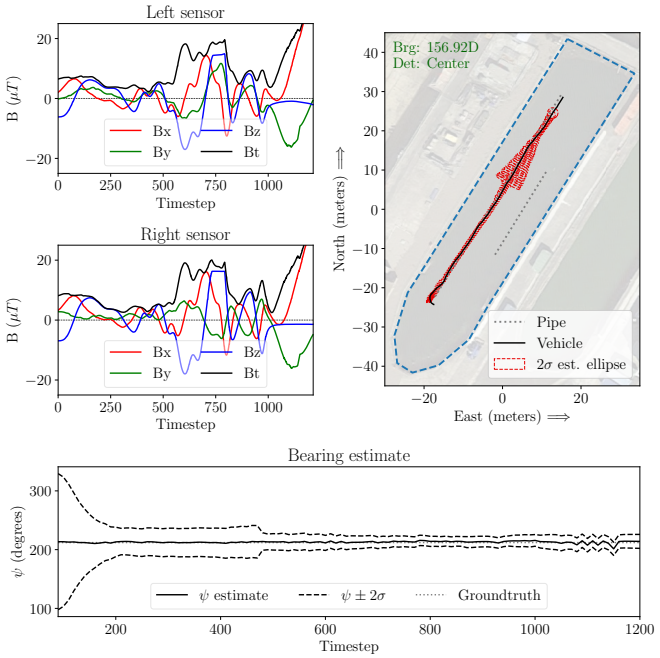

Fig. 8: The covariance ellipse increases initially since the Kalman filter gets initialized but a detection above the pipe is not made due to total magnetic below threshold, B_{thresh}. Increases initially because of large covariance in relative bearing of the pipe. ASV Motion: N-E to S-W from fully buried to exposed.

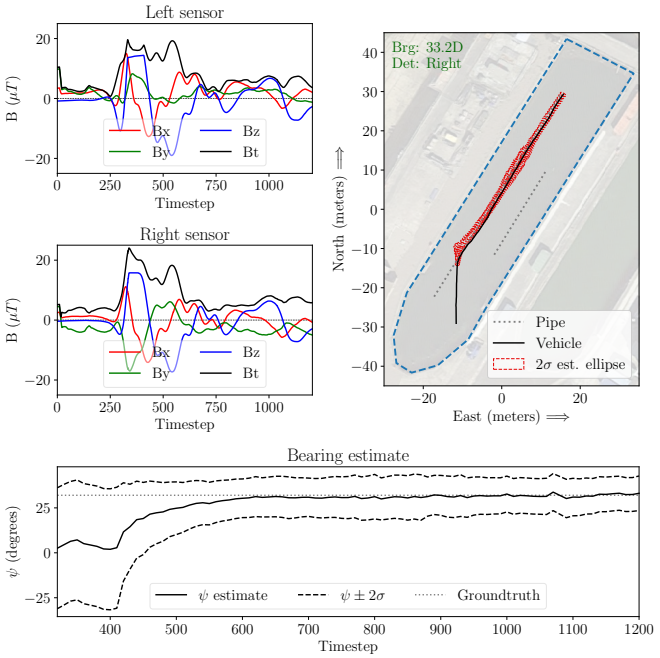

Fig. 9: Results when the pipe is crossing the pipe. Turning and successive 'centre' detections makes the estimate converge faster. ASV Motion: towards north, then towards N-E crossing pipe at exposed then going to buried section.

and then goes above the pipe. Filter converges quickly as a large number of pipe detections are made.

VI. Conclusion

We've presented an approach to track subsea pipelines using only magnetometer-based detections. The proposed method is very handy when a subsea pipeline is being tracked using a visual or profiling sensor and goes into burial. The magnetometer-based tracker can keep a good estimate of the pipe as long as the vehicle is controlled well from these estimates and does not lose track. We've also done observability analysis for the proposed Kalman filter to make sure it is observable and is able to estimate optimally given the detections. In future we would like to extend the filter to be used with other sensor modalities such as tracking in conjunction with a Multibeam Echosounder.

ACKNOWLEDGMENT

The authors would like to thank Kawasaki Heavy Industries for supporting this project and data collection. The authors would also like to thank Hydrason Solutions for arranging trails for data gathering at Blyth, UK and Shimadzu Corporation for supplying with magnetometers used in collecting data for this work.

References

[1] R. L. Wernli, "Auv commercialization-who's leading the pack?," in *OCEANS 2000 MTS/IEEE Conference and Exhibition*, vol. 1, pp. 391–395, IEEE, 2000.

[2] L. L. Whitcomb, "Underwater robotics: Out of the research laboratory and into the field," in *Robotics and Automation, 2000. Proceedings. ICRA'00. IEEE International Conference on*, vol. 1, pp. 709–716, IEEE, 2000.

[3] J. Evans, Y. Petillot, P. Redmond, M. Wilson, and D. Lane, "AUTOTRACKER: AUV embedded control architecture for autonomous pipeline and cable tracking," in *OCEANS 2003. Proceedings*, vol. 5, pp. 2651–2658, IEEE, 2003.

[4] M. Ortner and L. G. Coliado Bandeira, "Magpylib: A free python package for magnetic field computation," *SoftwareX*, submitted 01/2020.

[5] S. Breiner, "Applications manual for portable magnetometers," *Geometrics, San Jose*, 1999.

[6] Z.-Y. Guo, D.-J. Liu, Q. Pan, and Y.-Y. Zhang, "Forward modeling of total magnetic anomaly over a pseudo-2d underground ferromagnetic pipeline," *Journal of Applied Geophysics*, vol. 113, pp. 14–30, 2015.

[7] D. Zhao, Z. Guo, J. Du, Z. Liu, W. Xu, and G. Liu, "Geometric modeling of underground ferromagnetic pipelines for magnetic dipole reconstruction-based magnetic anomaly detection," *Petroleum*, 2019.

[8] W.-M. Tian, "Integrated method for the detection and location of underwater pipelines," *Applied Acoustics*, vol. 69, no. 5, pp. 387–398, 2008.

[9] W. Naeem, R. Sutton, and S. Ahmad, "Pure pursuit guidance and model predictive control of an autonomous underwater vehicle for cable/pipeline tracking," in *Proceedings-Institute of Marine Engineering Science and Technology Part C Journal of Marine Science and Environment*, pp. 25–35, THE INSTITUTE OF MARINE ENGINEERING, SCIENCE AND TECHNOLOGY, 2004.

[10] A. Chulliat, S. Macmillan, P. Alken, C. Beggan, M. Nair, B. Hamilton, A. Woods, V. Ridley, S. Maus, and A. Thomson, "The us/uk world magnetic model for 2015-2020," 2015.

[11] V. Bharti, D. Lane, and S. Wang, "Robust subsea pipeline tracking with noisy multibeam echosounder," in *2018 IEEE/OES Autonomous Underwater Vehicle Workshop (AUV)*, pp. 1–5, IEEE, 2018.

[12] Z. Chen, "Local observability and its application to multiple measurement estimation," *IEEE transactions on Industrial Electronics*, vol. 38, no. 6, pp. 491–496, 1991.